ISSN: 2278-4632
Vol-13, Issue-02, No.01, February 2023

Four Port Converter based on FLC & ANFIS Controller

S. ANUSHA Assistant Professor (Adhoc) ,
B. ANUSHA PG Scholar
Dept. of Electrical and Electronics Engineering (Power & Industrial Drives),
Jawaharlal Nehru Technological University College of Engineering Anantapur, India
bhumireddyanusha999@gmail.com, *sankranthi.anusha2425@gmail.com*

ABSTRACT
This paper presents the implementation of Fuzzy Logic Controller (FLC) & ANFIS Controller for a modified structure of non-isolated four-port (two input and two output ports) power electronic interfaces that can be utilized in electric vehicle (EV) applications. The main feature of this converter is its ability to accommodate energy resources with different voltage and current characteristics. The suggested topology can provide a buck and boost output simultaneously during its course of operation. The proposed four-port converter (FPC) is realized with reduced component count and simplified control strategy which makes the converter more reliable and cost-effective. Besides, this converter exhibits bidirectional power flow functionality making it suitable for charging the battery during regenerative braking of an electric vehicle. The steady-state and dynamic behaviour of the converter are analysed and a control scheme is presented to regulate the power flow between the diversified energy supplies. A small-signal model is extracted to design the proposed converter. The validity of the converter design and its performance behaviour is verified.

INDEX TERMS--Multi-port converter, electric vehicle, bidirectional dc/dc converter, battery storage, regenerative charging, Fuzzy Logic Controller, ANFIS Controller.

INTRODUCTION

Increasing environmental pollution, the rapid rise in fuel cost, global warming, and depletion of fossil fuels have led to the development of advanced vehicle technologies. Therefore automobile industries have started manufacturing eco-friendly electric (EV) & hybrid electric vehicles (HEV). In such vehicles, the motor drive system is an important component. An efficient power electronic converter is required to propel the motor drive system. In the case of EV, this power electronic converter must possess the bidirectional capability to interface the energy resources with battery and motor drive systems. Numerous research work has been reported by the researchers in the literature on power electronic interfaces for EV systems. Different topologies of non-isolated three-port converter synthesized from dual input (DIC) or dual output (DOC) converter along with the single input single output (SISO) converter is dealt in [1]. A step-up converter combining the features of KY converter and buck-boost converter with a high voltage conversion ratio is presented in[2].

The method of improving the conversion efficiency using the interleaving concept in a double switch buck-boost converter is proposed [3]. A non-isolated boost converter with high voltage gain capable of balancing automatically under an unbalancing load condition is analyzed in [4]. Bang and Park [5] describe buck cascaded buck-boost power factor correction converter for wide input voltage variations. The above-mentioned converters are unidirectional with the SISO configuration. A non-isolated bidirectional dc/dc converter in [6] is a SISO model that uses four active switches. A comparison of two different bidirectional converters such as cascaded buck- boost capacitor in the middle and cascaded buck-boost inductor in the middle is carried out in [7].

To achieve high power density and enhance efficiency, zero-voltage transition three-level dc/dc converter with the soft switching feature is proposed [8]. The converter in [9] is a three-port bidirectional topology that uses three inductors and three active switches to produce either buck or boost output. Different structures of parallel buck-boost converters, converters with two modules of super capacitors and their power management control strategies are well investigated in [10].

A Multi-port energy converter in [11] employs a single leg active switching element for the multi-

ISSN: 2278-4632
Vol-13, Issue-02, No.01, February 2023

functional operation to regulate and manage the output power.

When comparing the above-said converter with the basic buck-boost converter, it uses more passive elements. A bidirectional high gain step-up/down dc converter in [12] which has been realized as a non-isolated structure has an in-built DC transformer which increases the size of the converter. The single switch buck-boost topology presented in operates in SISO mode and it inherits the features of CUK converters and supersedes the problems encountered in KY converter. Non-isolated multi- input multi-output dc/dc converters presented in is a boost converter meant for photovoltaic applications with unidirectional power flow.

The setback of a multi-input single-output n-stage converter in [17], [18] is that only (n-1) stages do the buck-boost operation and the nth stage operates as a boost converter with power transferredfrom source to load always. The circuit configuration in [19], [20] is designed with switched capacitor technique for multiple inputs applications. Here, the number of active and passive components used in this configuration equals the number of input sources, which in turn increasesthe circuit structure and control complexity. The utilization of single inductor based non-isolated multi-port converter proposed in [21], [22] is limited to low power applications one active switch for integrating diversified load devices. Multiport dc/dc converter in [23] is an isolated bidirectionalconverter. A Multi-winding transformer in it which helps in transferring the power increases the size of the converter. Different structures of multiport bidirectional dc/dc converters are derived with the combination of dc-link and magnetic coupling [24]. Fully directional universal dc/dc converter [25] operates as a SISO converter. A dual input dual output converter suitable for the hybrid electric vehicle is proposed [26].

It has the basic disadvantage of battery power not being boosted across the load. A solar power aided EV with battery backup has been in [27]. To catalyze the energy between the battery and solarin the above EV a dc/dc converter structure has been presented. The number of switches in this converter varies based on the number of battery modules (Say if there exists ‘n’ no. of battery modules, then the system requires ‘2n’ numbers of switches for effective operation). For effective power management between the ultra-capacitor and battery and to suppress the issues such as overcharging of ultra-capacitor and high battery current during peak power, a fuzzy logic control based energy management strategy has been proposed [28].

The major contribution of this paper is to propose a single-stage transformer less four-port (FPC) bidirectional buck-boost converter with only three switches. Compared with the topologies presented in the literature , the proposed converter has advantages such as a modular structure withreduced component count and integration of diversified sources in the input with different voltage- current characteristics. Apart from the above-said features, the proposed converter can provide output less than the minimum input voltage (buck) or greater than the maximum input voltage (boost). The reduction of switching losses improves the efficiency of the proposed converter.

PERFORMANCE ANALYSIS OF MULTIPORT BUCK-BOOST CONVERTER:

A.STRUCTURE OF FPC TOPOLOGY:

The use of a single energy resource cannot meet the load demand due to input power variations and dynamic load in the electric vehicular system. Therefore, the hybridization of arbitrary energyresources is required. This manuscript focuses on synthesizing a converter topology that could interface various energy resources with the drive train of a vehicle. Figure 1 (a) and (b) depict therole of power electronic interface in the power system of an electric vehicle system.

ISSN: 2278-4632
Vol-13, Issue-02, No.01, February 2023

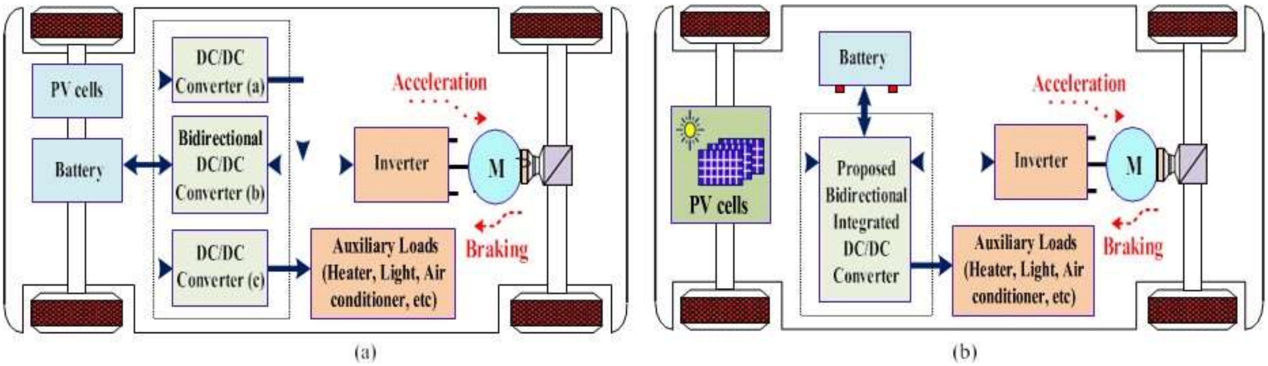

Fig.1 Block diagram of (a) Conventional converter (b) Proposed integrated four-port converter (FPC) interface in an electric vehicle system.

Figure 2 shows the proposed topology of a four-port (FPC) converter. Prominent features of the proposed converter are: , Bidirectional power flow capability , Individual power flow control between the sources , Easy design, control, and implementation process As shown in Figure 2 thepower flow between load and input sources is controlled by the controllable switches Q_1, Q_2, and
Q_3. As seen from Figures 3a to 3e five different states of operation can be considered for the proposed converter. The state 1 is a (single input dual output) SIDO state.

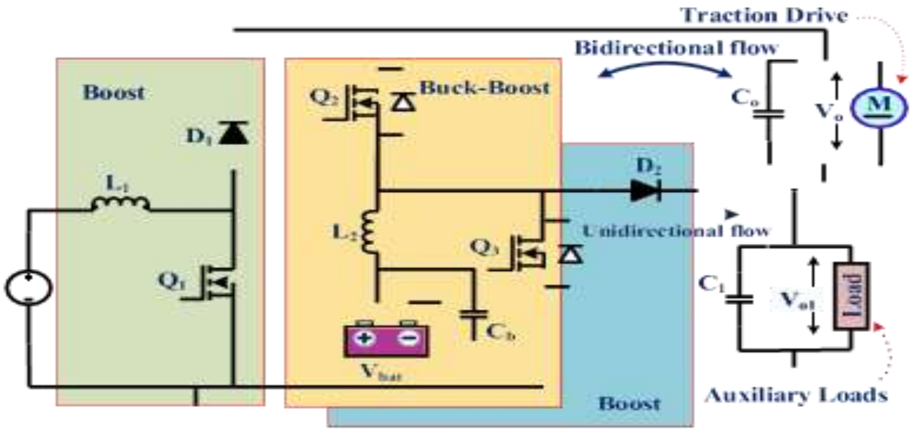

Fig.2 Topology diagram of four-port (FPC) converter

In this state (see Figure 3a), the drive train of EV (load) is powered by the power generated from PV. The battery in the proposed topology can be charged either from the input PV power or from the load (see Figure 3b & Figure 3e). In state 5, due to regenerative braking the energy returning from the load is stored in the battery. Due to low irradiation and if the PV is not able to generate the power, the battery discharges to meet the entire load requirement (see Figure 3c). During peak power demand, the battery unit and PV provide the necessary power to drive train. The converter then operates in the DIDO state (see Figure 3d). Switching schemes of the proposed converter and equivalent circuits under different operating states are depicted in Figures 4 & 5 respectively.

ISSN: 2278-4632
Vol-13, Issue-02, No.01, February 2023

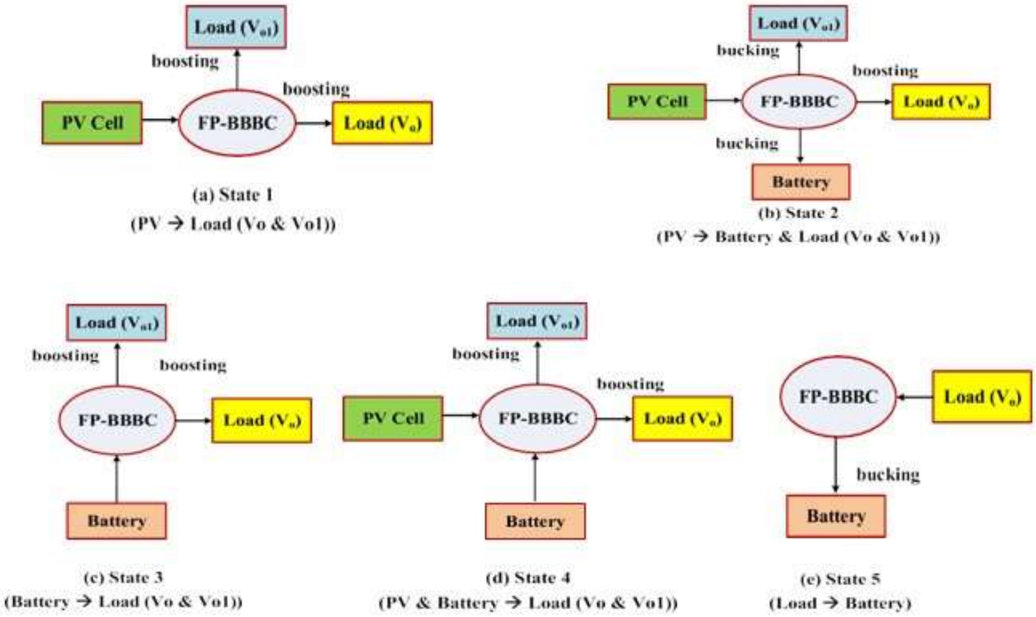

Fig.3 a) State 1(boost), b) State 2 (buck & boost), c) State 3 (boost), d) State 4 (boost), e) State 5 (buck)

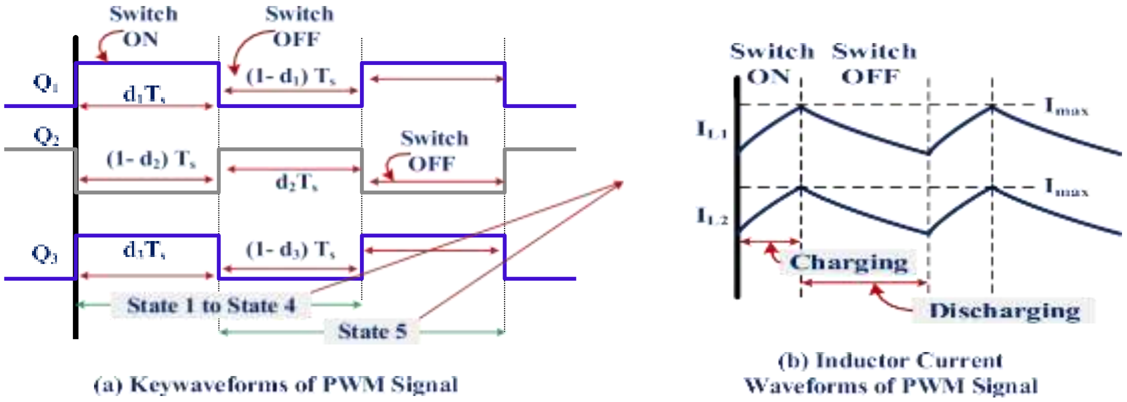

Fig.4 State of operation of proposed FPC

B. OPERATING MODES -STATE OF OPERATION:

1) STATE 1-SIDO (SINGLE INPUT DUAL OUTPUT) STATE OF THE CONVERTER (POWER TRANSFER FROM PV (VDC) TO LOAD):

In this state, PV transfers the power individually to the load. The Switching schemes of various operating devices are shown in Table 2. Switches Q_1 and $Q_3$are turned ON and, Q_2 is turned OFF, during the time interval 0 to d_1T_s. While considering $V_{pv} > V_{bat}$ (see Figure 5 (a) and (b)), the voltage V_{pv} appears across the inductor L_1, resulting in the rise of inductor current with the positive slope. During time interval d_1T_s. to Ts, switches Q_1 , Q_3 are turned off and Q_2 is turned on. Energy stored in inductor L_1 during the previous time interval d1Ts is discharged to the output capacitor through the diode D_1. Here T_s. is the switching time period.

ISSN: 2278-4632
Vol-13, Issue-02, No.01, February 2023

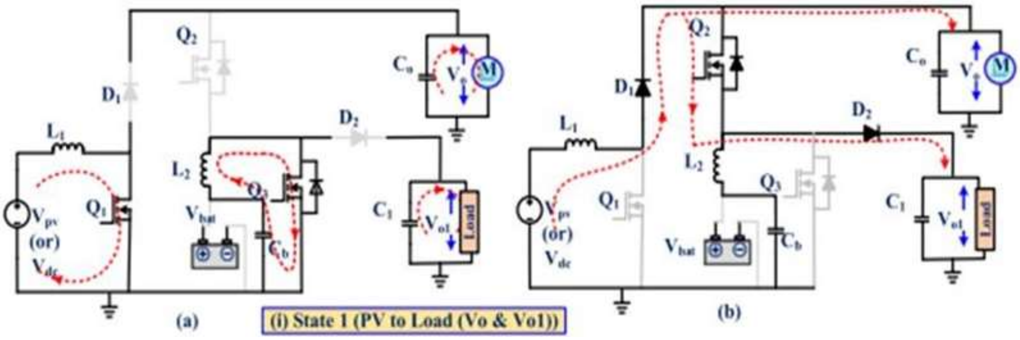

Fig.5 State1 (PV to Load (V_0 & V_{01}))

$$V_0 = \frac{1}{1-d_1} V_{pv} \tag{1}$$

$$V_{01} = \frac{1}{1-d_1} V_{pv} \tag{2}$$

2) STATE 2- SITO (SINGLE INPUT THREE OUTPUT) STATE OF THE CONVERTER (POWER TRANSFER FROM PV TO BATTERY AND LOAD):

Operation in this state is similar to state 1. When the battery needs to be charged from PV (see Figure 5 (c) and (d)), Q_2 operates with $d_2 < 0.5$ to charge the battery. Q_3 operates similarly as that of Q_1 with $d_1 > 0.5$ to produce boosted output across the load. Voltages V_{bat}, V_{pv}, and V_0, V_{01} are related by the equation.

$$V_0 = \frac{1}{1-d_1} V_{pv} \tag{3}$$

$$V_{01} = d_2 V_{pv} \tag{4}$$

$$V_{bat} = d_2 V_{pv} \tag{5}$$

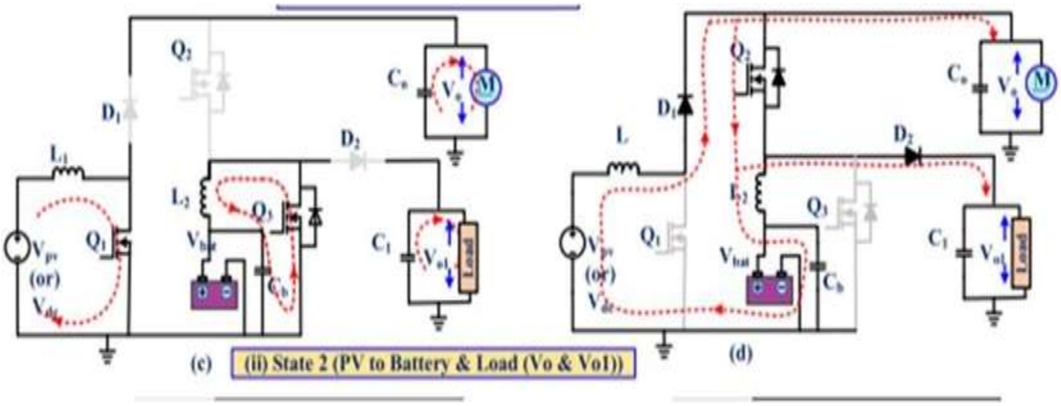

Fig.5 State 2 (PV to Battery & Load (V_0 & V_{01}))

3) STATE 3 - SIDO STATE OF THE CONVERTER (POWER TRANSFER FROM THE BATTERY)

In this state, the energy stored in the battery is transferred to the load. During the time interval 0 to d_3T_s , discharging action of the battery causes the inductor current i_{L2} to rise linearly. Between the intervals d_3T_s to T_s , the current i_{L2} decreases with a negative slope. ON-OFF state of switch Q_3 provides a boosted output across the drive train. As Q_1 does not take part in transferring the energy from battery to as Q_1 does not take part in transferring the energy from battery to the load, it is kept in OFF condition throughout the state of operation (see Figure 5 (e) and (f)). The output voltage

ISSN: 2278-4632
Vol-13, Issue-02, No.01, February 2023

across the load due to discharging the battery is given as

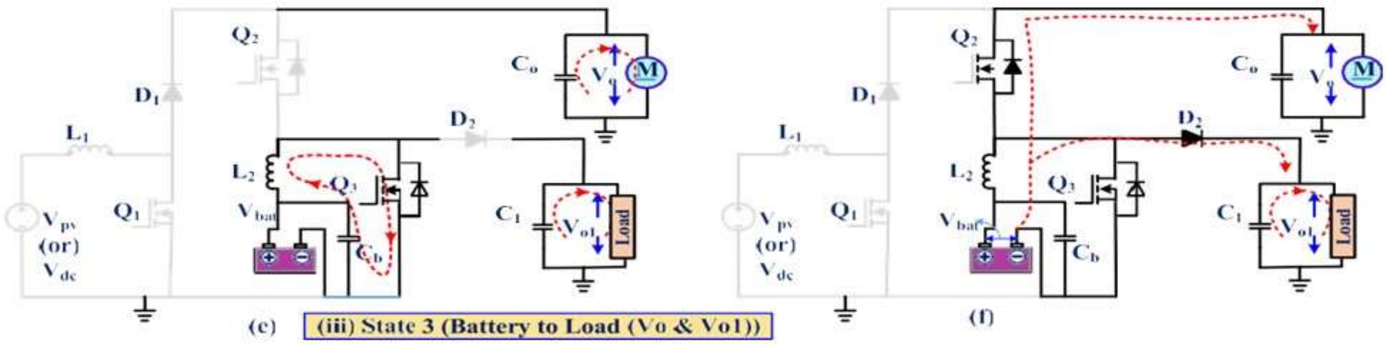

Fig.5 State 3 (Battery to Load (V_0 & V_{01}))

$$V_0 = \frac{1}{1-d_3} V_{bat} \quad (6)$$

$$V_{01} = \frac{1}{1-d_3} V_{bat} \quad (7)$$

4) STATE 4 – DIDO (DUAL INPUT DUAL OUTPUT) STATE OF THE CONVERTER (POWER TRANSFER FROM PV AND BATTERY)

When the power demand from EV is high, the battery and PV supply, power to meet the demand (see Figure 5 (g) and (h)). During time interval 0 to $d_1 T_s$ gated switches Q_1 and Q_3 charge the inductor and cause the currents i_{L1} and i_{L2} to rise linearly. Q_2 is provided with the complimentary gate signal at this interval. On the other hand during the off period of switches Q_1 , Q_3 the inductor currents i_{L1} and i_{L2} decrease with the negative slope. Thus boosted power from both battery and PV is delivered to the load via diodes D_1 and D_2. Net output voltage due to the power delivery of both the sources can be determined from Eqs.(8):

$$V_0 = \frac{1}{1-d_1} V_{pv} \text{ , (or) } \quad V_0 = \frac{1}{1-d_3} V_{bat} \quad (8)$$

$$V_{01} = \frac{1}{1-d_1} V_{pv} \text{ , (or) } \quad V_{01} = \frac{1}{1-d_3} V_{bat} \quad (9)$$

ISSN: 2278-4632
Vol-13, Issue-02, No.01, February 2023

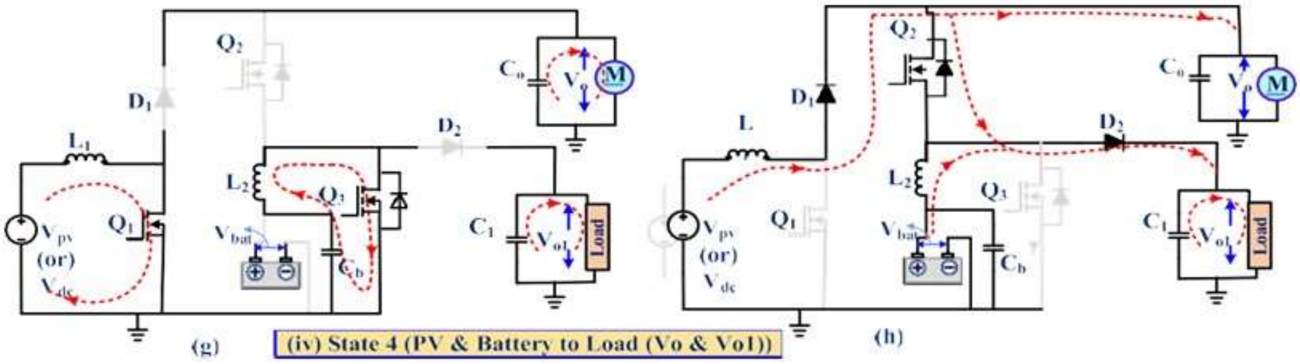

Fig.5 State 4 (PV & Battery to Load (V_0 & V_{01}))

5) STATE 5 - SIDO STATE OF THE CONVERTER (POWER TRANSFER FROM LOAD TO BATTERY)

During regenerative braking, the kinetic energy stored in the drive train is fed back to the battery (see Figure 5 (i) and (j)). The switching sequence of this state is given as follows: Q_1 is permanently in the off condition; Q_2, Q_3 is turned ON and Q_2 is turned OFF. The ON-OFF state of Q_2 along with Q_2 charges the battery.

$$V_{bat} = d_2 V_0 \tag{10}$$

In same state, the battery is supplied by the second output through regenerative braking power. The control relation is derived as,

$$V_{01} = d_3 V_0 \tag{11}$$

C.CONVERTER FAULT ANALYSIS:

The converter fault condition is investigated Considering 4 different cases :-

Case-1: If switch Q_1 opens, the boosted PV power will not be available as the diode D_1 will be reverse biased. The converter works in SIMO state and continues to power the loads with the available battery power. At, the same time the regenerative power if available will charge the battery with the aid of switches Q_2 and Q_3.

Case-2: If switch Q_2 opens, the PV module will not be able to power the auxiliary loads and the battery cannot be charged during regenerative braking. However, the PV modules will be able to drive the traction drive with its available power and the converter works in SISO state.

Case-3: If switch Q_3 opens, the charging and discharging action will be affected. Battery will not be able to deliver boosted output across the loads?

Case-4 Due to switching (ON-OFF) action, switch Q_1 delivers boosted output across the loads through diode D_1. But if diode D_1 opens, then the load will not be delivered with boosted output and there will be circulating current through the inductor L_1 and the switch which in turn will generate heat in the loop. Similarly, if the diode D_2 opens, there will not any power supplied through the diode D_2 to the load.

III. DYNAMIC MODELING:

A proper control scheme is required to fix the duty cycles of an individual switch in the converter to regulate the output voltages, the charging, and discharging actions of the battery. Therefore, to design such controllers, dynamic modeling of the converter using a small-signal model needs to be obtained. The state-space average model of the four-port converter is derived based on the state-space description of the converter in each switching state. Following are the steps involved in deducing the average model.

Derivation of state-space equation during open close condition of switches, Averaging the deduced state equations, Perturbation, Matrix creation.

To obtain the small-signal model, the current through the inductors and voltage across the

ISSN: 2278-4632
Vol-13, Issue-02, No.01, February 2023

capacitors are assumed as state variables. As five operating states of the presented converter use different combinations of the two input sources and produce either buck, boost, or buck-boost outputs simultaneously five different models can be obtained. State variables in equation (12), (13) and (14) consist of DC components (I, d, V) and perturbations (ˆi, dˆ, v). Perturbations are assumed to ˆ have small variations over one switching period. Replacing the state parameters with the sum of steady- state parameters and perturbation values, the following constraints can be derived.

$$\begin{aligned} i_{L1} &= I_{L1} + \hat{\imath}_{L1} \\ i_{L2} &= I_{L2} + \hat{\imath}_{L2} \\ v_0 &= V_0 + \hat{v}_0 \end{aligned} \tag{12}$$

$$\begin{aligned} v_{01} &= V_{01} + \hat{v}_{01} \\ v_{bat} &= V_{bat} + \hat{v}_{bat} \end{aligned} \tag{13}$$

$$\begin{aligned} d_1 &= d_1 + \hat{d}_1 \\ d_2 &= d_2 + \hat{d}_2 \\ d_3 &= d_3 + \hat{d}_3 \end{aligned} \tag{14}$$

A. STATE 1 (V_{pv}→ LOAD [BOOST OPERATION])

As the converter is considered to be operating in CCM, the switches (see Figure 5 (a) and (b)) Q_1 is ON, Q_2 is OFF for a period of d_1T_s , and Q_1 is OFF, Q_2 is ON for a period (1- d_1T_s). Substituting the perturbations, it is possible to obtain.

$$\frac{d(\hat{v}_0)}{dt} = \left(\frac{1-d_1}{c_0}\right)\hat{\imath}_{L1} - \left(\frac{\hat{d}_1}{c_0}\right)I_{l1} - \left(\frac{1}{c_0\,r_0}\right)\hat{v}_0 \tag{15}$$

$$\frac{d(\hat{v}_{01})}{dt} = \left(\frac{1-d_1}{c_1}\right)(\hat{\imath}_{L1} + \hat{\imath}_{L2}) - \left(\frac{\hat{d}_1}{c_1}\right)(I_{L1} + I_{L2}) - \left(\frac{1}{c_1\,r_1}\right)\hat{v}_{01} \tag{16}$$

$$\hat{d}_1 I_{L1} = (1-d_1)\,\hat{\imath}_{L1} - \left(c_0 + \frac{1}{r_0}\right)\hat{v}_0 \tag{17}$$

$$\hat{d}_1 I_{L1} = (1-d_1)\,(\hat{\imath}_{L1} + \hat{\imath}_{L2}) - \left(c_1 + \frac{1}{r_1}\right)\hat{v}_{01} \tag{18}$$

$$\frac{1}{\hat{d}_1}\begin{bmatrix} \hat{\imath}_{L1} \\ \hat{v}_0 \\ (\hat{\imath}_{L1} + \hat{\imath}_{L2}) \\ \hat{v}_{01} \end{bmatrix} = \begin{bmatrix} L_1 & (1-d_1) & 0 & 0 \\ (1-d_1) & \left(c_0 + \frac{1}{r_0}\right) & 0 & 0 \\ 0 & 0 & (L_1 + L_2) & (1-d_1) \\ 0 & 0 & (1-d_3) & \left(c_1 + \frac{1}{r_1}\right) \end{bmatrix}^{-1} \times \begin{bmatrix} I_{L1} \\ V_0 \\ (I_{L1} + I_{L2}) \\ V_{01} \end{bmatrix} \tag{19}$$

B. STATE 2 (V_{pv} → V_{bat} & LOAD [BUCK & BOOST])

In this state, Q_1 and Q_3 are kept ON and Q_2 remains in the OFF state as in Figure 5 (c) and (d). Incorporating the perturbations are given as,

$$\frac{d_1(V_0+\hat{v}_0)}{dt} = \left(\frac{1-d_1-\hat{d}_1}{c_0}\right)(I_{L1} + \hat{\imath}_{L1}) - \left(\frac{1}{c_0 r_0}\right)(V_0 + \hat{v}_0) \tag{20}$$

$$\frac{d_2(V_{01}+\hat{v}_{01})}{dt} = \left(\frac{1}{c_0}\right)(I_{L2} + \hat{\imath}_{L2}) - \left(\frac{1}{c_1 r_1}\right)(V_{01} + \hat{v}_{01}) \tag{21}$$

$$\frac{d_2(V_{bat}+\hat{v}_{bat})}{dt} = \left(\frac{1}{c_b}\right)(I_{L2} + \hat{\imath}_{L2}) - \left(\frac{1}{c_b}\right)(V_{bat} + \hat{v}_{bat}) \tag{22}$$

$$\frac{1}{\hat{d}_1\&\hat{d}_2\&\hat{d}_3}\begin{bmatrix}\hat{\imath}_{L1}\\ \hat{\imath}_{L2}\\ \hat{v}_0\\ \hat{v}_{bat}\\ \hat{v}_{01}\end{bmatrix} = \begin{bmatrix} L_1 & 0 & (1-d_1) & 0\\ 0 & 0 & 0 & (-d_2)\\ (1-d_1) & 0 & -\left(c_0+\frac{1}{r_0}\right) & 0\\ 0 & -1 & 0 & -1\\ (1-d_3) & 0 & -\left(c_1+\frac{1}{r_1}\right) & 0\end{bmatrix}^{-1}\begin{bmatrix}V_0\\ V_{bat}\\ V_{01}\\ I_{L1}\\ I_{L2}\end{bmatrix} \tag{23}$$

C. STATE 3 (V_{bat}→ LOAD [BOOST])

During this state, the switch Q_3 is ON and Q_2 is OFF condition, inductor L_2 is charged. Switch Q_3 is OFF and Q_2 is ON, inductor L_2 is discharged from Figure 5 (e) and (f). Small-signal equations that can be deduced are

$$\frac{1}{\hat{d}_3}\begin{bmatrix}\hat{\imath}_{L2}\\ \hat{v}_{01}\\ \hat{v}_0\end{bmatrix} = \begin{bmatrix} L_2 & (1-d_3) & 0\\ (1-d_3) & \left(c_1+\frac{1}{r_1}\right) & 0\\ 0 & (1-d_3) & \left(c_0+\frac{1}{r_0}\right)\end{bmatrix}^{-1} \times \begin{bmatrix}I_{L2}\\ V_{01}\\ V_0\end{bmatrix} \tag{24}$$

D. STATE 4 (V_{pv} and V_{bat} → LOAD [BOOST])

As state 4 combines the operation (see Figure 5 (g) and (h)) of state 1 and state 3, the average model of the converter with the switching sequence shown in Table 2 can be derived as

$$\frac{1}{\hat{d}_1\&\hat{d}_3}\begin{bmatrix}\hat{\imath}_{L1}\\ \hat{v}_0\\ \hat{\imath}_{L2}\\ \hat{v}_{01}\end{bmatrix} = \begin{bmatrix} L_1 & (1-d_1) & 0 & 0\\ (1-d_1) & \left(c_0+\frac{1}{r_0}\right) & 0 & 0\\ 0 & 0 & L_2 & (1-d_3)\\ 0 & 0 & (1-d_3) & \left(c_1+\frac{1}{r_1}\right)\end{bmatrix}^{-1} \times \begin{bmatrix}I_{L1}\\ V_0\\ I_{L2}\\ V_{01}\end{bmatrix} \tag{25}$$

E. STATE 5 (LOAD → V_{bat} [BUCK AND BOOST])

ISSN: 2278-4632
Vol-13, Issue-02, No.01, February 2023

$$\frac{d(I_{L2}+\hat{\imath}_{L2})}{dt} = \left(\frac{d_2-\hat{d}_2}{L_2}\right) V_{brake} - \left(\frac{1}{L_2}\right)(v_{bat} + \hat{v}_{bat}) \tag{26}$$

$$\frac{d(V_0 + \hat{v}_0)}{dt} = \left(\frac{I_{L2} + \hat{\imath}_{L2}}{C_b}\right) - \left(\frac{v_{bat} + \hat{v}_{bat}}{C_b}\right) \tag{27}$$

$$\frac{d(\hat{\imath}_{L2})}{dt} = -\frac{v_{bat}}{L_2} - \frac{\hat{v}_{bat}}{L_2} \tag{28}$$

$$\frac{d(\hat{V}_{bat})}{dt} = \left(\frac{I_{L2} + \hat{\imath}_{L2}}{C_b}\right) - \left(\frac{\hat{v}_{bat}}{C_b}\right) \tag{29}$$

$$\frac{1}{\hat{d}_2}\begin{bmatrix}\hat{\imath}_{L2}\\ \hat{v}_{bat}\end{bmatrix} = \begin{bmatrix}-L_2 & -1\\ -1 & (1+C_b)\end{bmatrix}^{-1}\begin{bmatrix}I_{L2}\\ V_{bat}\end{bmatrix} \tag{30}$$

This state can be called as a regenerating state as the load power is negative. To store the regenerative braking energy in the battery, Q_1 is kept OFF, Q_2, and Q_3 are controlled as shown in Figure 5 (i) and (j). During regenerative operation, since the output voltage is greater than V_{pv}, the converter operates in buck mode and charges the battery. Averaging the state equations over one period, the small-signal model can be deduced as in equation below:

 ISSN: 2278-4632
Vol-13, Issue-02, No.01, February 2023

FUZZY LOGIC CONTROLLER:

Fuzzy Logic Controller (FLC) is a complex mathematical method that allows solving difficult simulated problems with many inputs and output variables.Fuzzy Logic Controller works with imprecise inputs,it does not need an accurate mathematical model and it can handle nonlinearity well.Fuzzzy Logic System is more robust compared to the conventional nonlinear controller.The operation of FLC has 4 classifications namely, Fuzzification ,Rule base, Inference engine and De-Fuzzification.

Fuzzification:

Fuzzification is the process of transforming a crisp set to fuzzy set or a fuzzy set to a fuzzier set. Membership function (MF) values are allotted to the linguistic variables, using five subsets: NB(negative big),NS(negative small),ZE(zero),PS(positive small),PB(positive big).These parameters are fuzzified fuzzified with the use of pre-defined input membership functions,which can have different shapes.The most common are: Triangular , bell , Trapezoidal , Sinusoidal , Exponential etc.The rule matrix is used to describe fuzzy sets and fuzzy operators in form of conditional statements.

Table.1 Fuzzy rules

ΔVpv*[o/p]	ΔVpv[i/p]					
		NB	NS	ZE	PS	PB
ΔPpv[i/p]	NB	PS	PB	NB	NB	NS
	NS	PS	PS	NS	NS	NS
	ZE	ZE	ZE	ZE	ZE	ZE
	PS	NS	NS	PS	PS	PS
	PB	NS	NB	PB	PB	PS

V_{pv} = Reference Voltage
ΔP_{pv} = Change in power
NB = Negative Big
NS = Negative Small
ZE = Zero
PB = Positive Big
PS = Positive Small

Inference method:

Inference engine mainly consists of fuzzy rule base and fuzzy implication sub-blocks.The inputs are now fuzzified and fed to the inference engine and the rule base is applied.The output fuzzy set is the identified using fuzzy implication method.Here we are using MIN-MAX fuzzy implication method.

Inference mechanism allows mapping given input to an output using fuzzy logic.It uses all pieces membership functions,logical operations and if-then rules.The most common types of inference systems are Mamdani and Sugeno method.

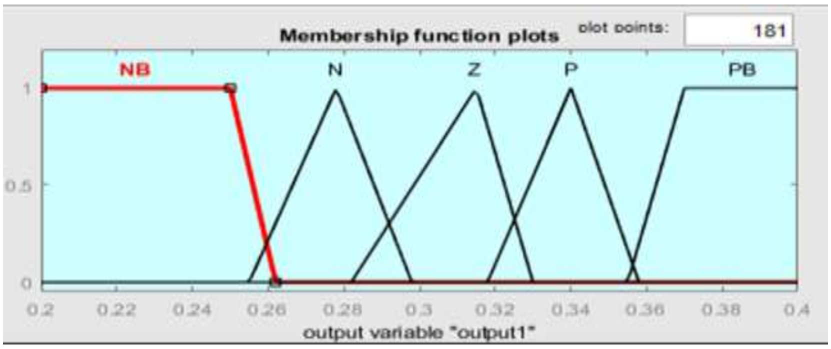

Fig.6 Output

De-Fuzzification:

De-Fuzzification is the process of transforming a fuzzy set in to a crisp set or a converting a fuzzy member in to a crisp member.There are several mathematical techniques available: Centroid , Bisector , Mean , Maximum and Weighted average.

Center of gravity is the method to compute the output of this FLC to generate the duty ratio(D).The center of gravity method is both very fast and simple method.

ISSN: 2278-4632
Vol-13, Issue-02, No.01, February 2023

SIMULATION MODELS & RESULTS USING FUZZY LOGIC CONTROLLER:

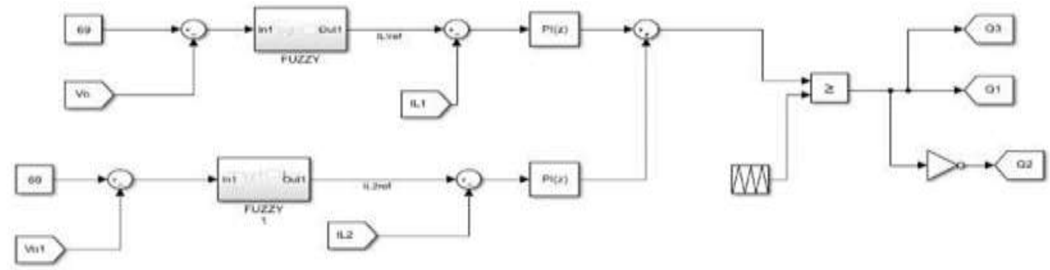

Fig. 7 Controlling Block of FUZZY Logic Controller

1) STATE 1-SIDO (SINGLE INPUT DUAL OUTPUT) STATE OF THE CONVERTER (POWER TRANSFER FROM PV (VDC) TO LOAD):

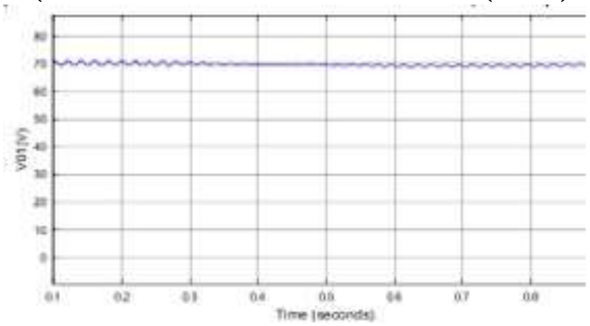

(a)

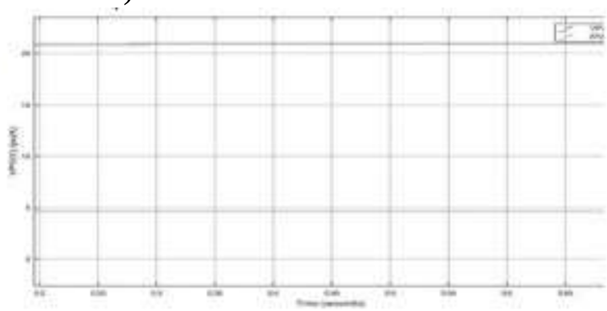

(b)

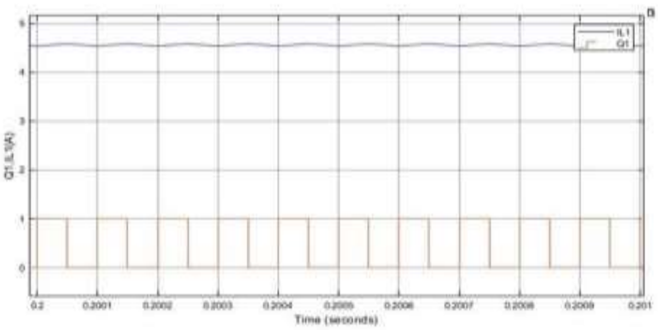

(c)

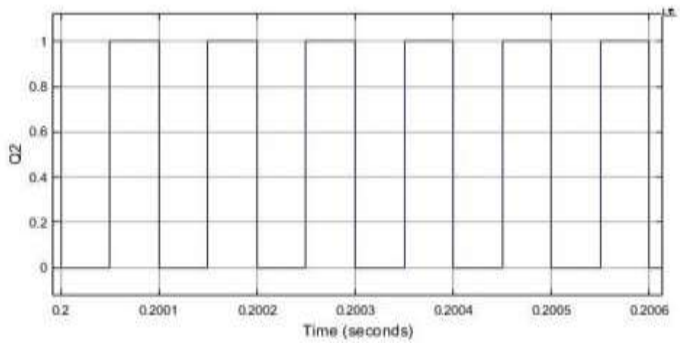

(d)

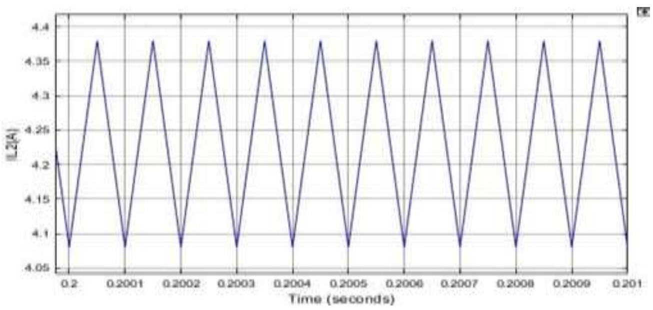

(e)

Fig. 8: (a) *Voltage*(V_{01}); **(b)** *Voltage*(V_{pv}) , *Current*(I_{pv}); **(c)** *Gate pulse*(Q_1) ,*Inductor Current*(I_{L1}); **(d)** *Gate Pulse*(Q_2); **(e)** *Inductor Current*(I_{L2})

2) STATE 2- SITO (SINGLE INPUT THREE OUTPUT) STATE OF THE CONVERTER (POWER TRANSFER FROM PV TO BATTERY AND LOAD):

ISSN: 2278-4632
Vol-13, Issue-02, No.01, February 2023

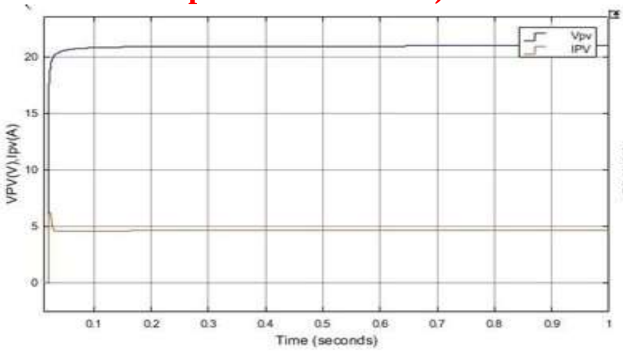

(a)

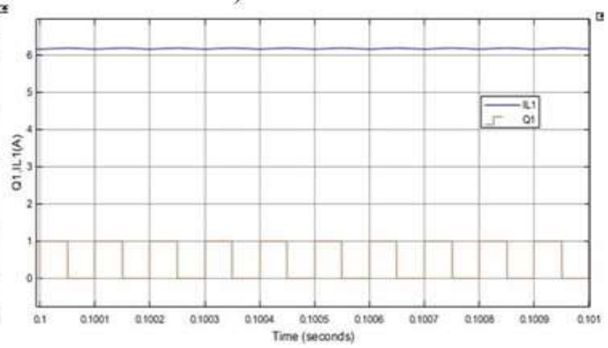

(b)

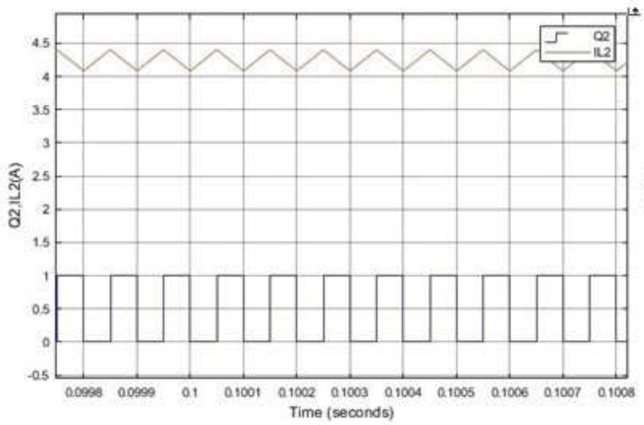

(c)

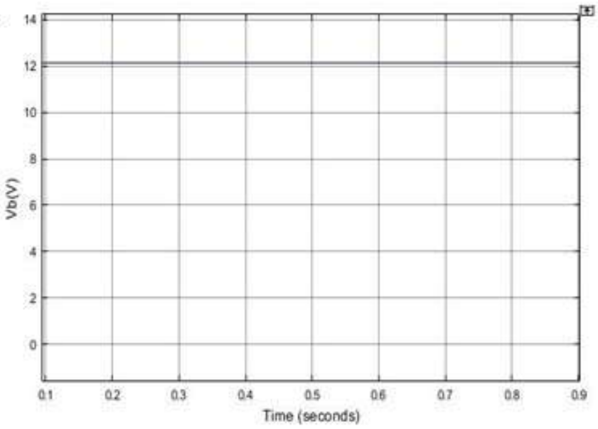

(d)

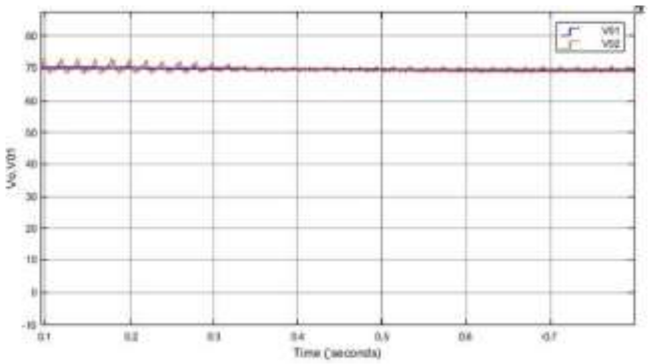

(e)

Fig. 9: (a) $Voltage(V_{pv}), Current(I_{pv})$**; (b)** $Inductor\ current(I_{l1})$**; (c)** $Gate\ pulse(Q_2), Inductor\ Current(I_{l2})$**; (d)** $Battery\ Voltage(V_{bat})$**; (e)** $Voltages(V_0), (V_{01})$

3) STATE 3 - SIDO STATE OF THE CONVERTER (POWER TRANSFER FROM THE BATTERY)

ISSN: 2278-4632
Vol-13, Issue-02, No.01, February 2023

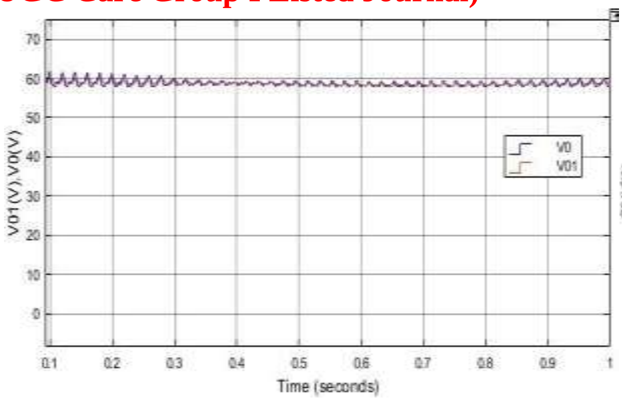

(a)

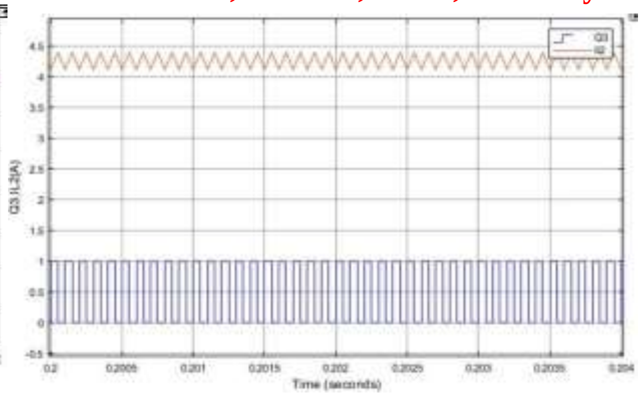

(b)

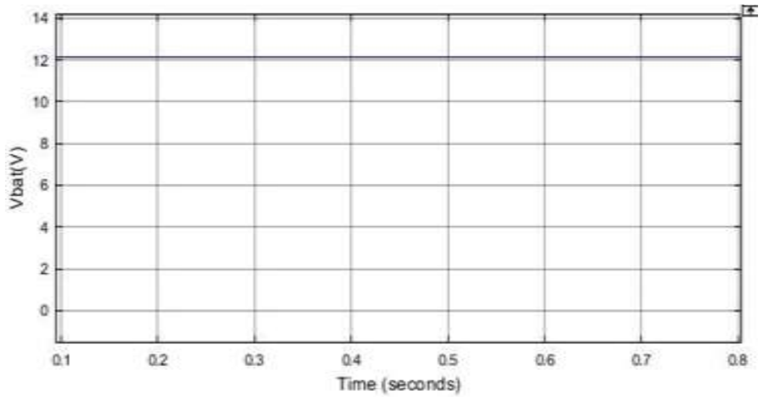

(c)

Fig. 10: (a) $Voltages(V_0)$, (V_{01}); **(b)** $Inductor\ Current(I_{l2})$; **(c)** $Battery\ Voltage(V_{bat})$

4) STATE 4 – DIDO (DUAL INPUT DUAL OUTPUT) STATE OF THE CONVERTER (POWER TRANSFER FROM PV AND BATTERY)

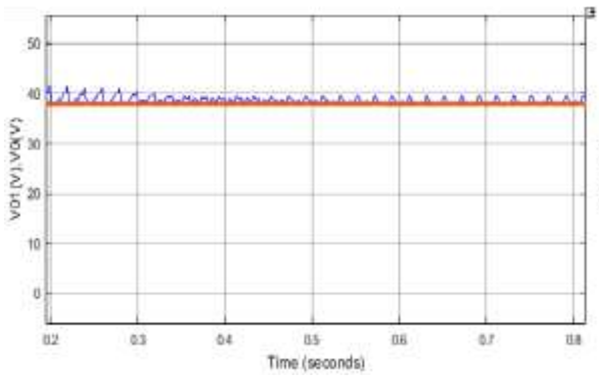

(a)

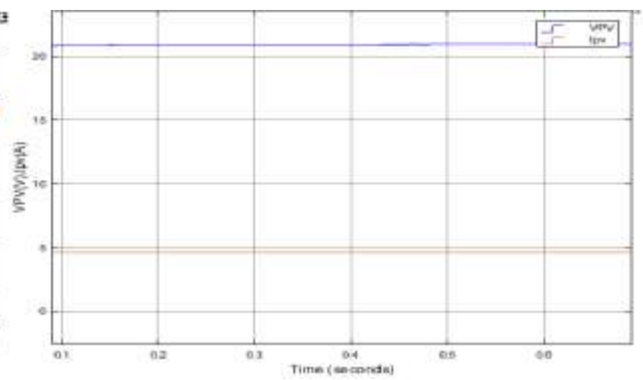

(b)

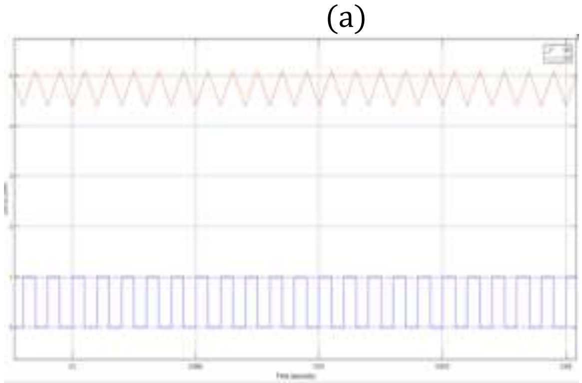

(c)

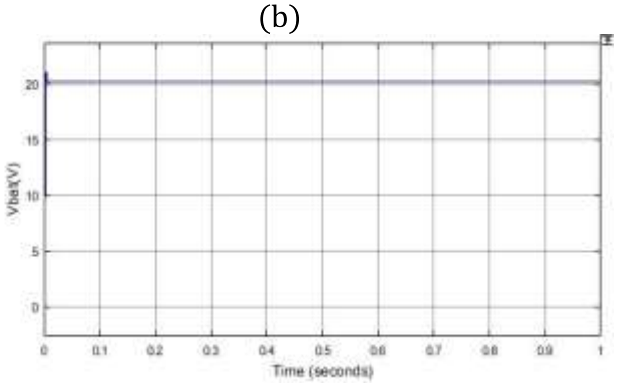

(d)

ISSN: 2278-4632
Vol-13, Issue-02, No.01, February 2023

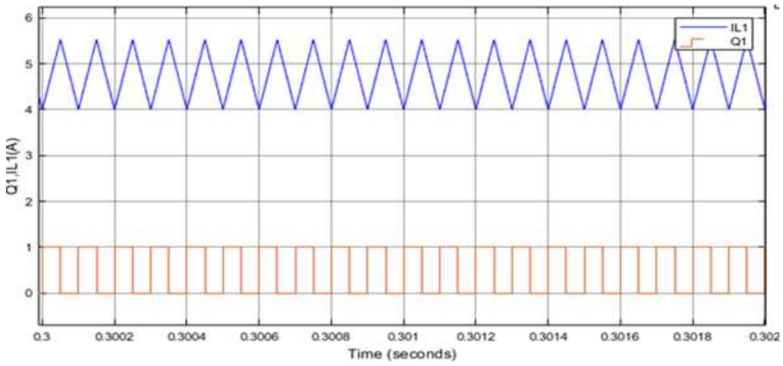

(e)

Fig. 11: (a) $Voltage(V_{01})$, (V_0); (b) $Voltage(V_{pv})$, $Current(I_{pv})$; (c) $Inductor\ current(I_{l2})$; (d) $Battery\ Voltage(V_{Bat})$; (e) $Inductor\ Current(I_{l1})$

5) STATE 5 - SIDO STATE OF THE CONVERTER (POWER TRANSFER FROM LOAD TO BATTERY)

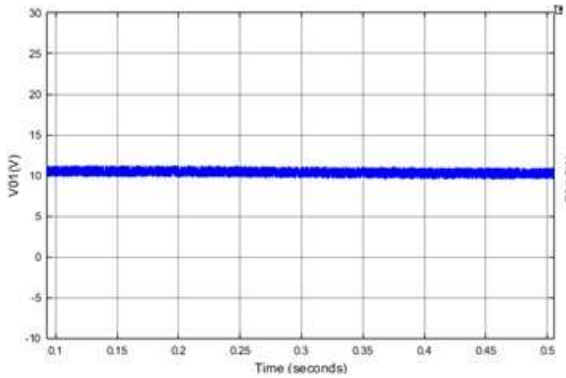

(a)

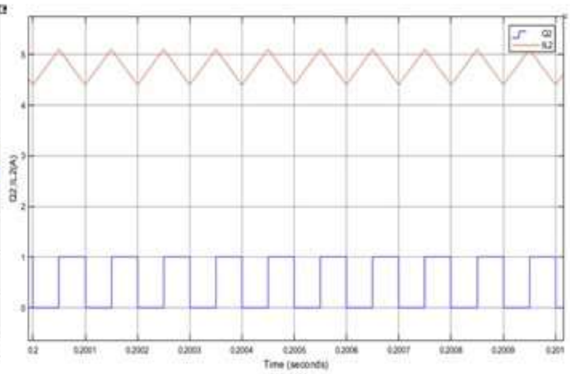

(b)

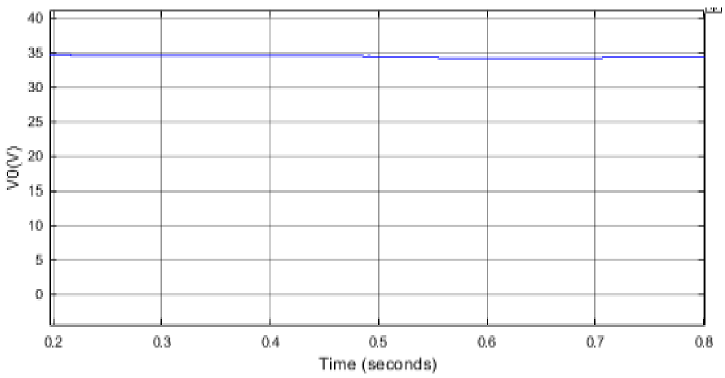

(c)

Fig. 12: (a) $Voltage(V_{01})$; (b)$Inductor\ Current(I_{l2})$; (c) $Voltage(V_0)$

ADAPTIVE NETWORK BASED FUZZY INFERENCE SYSTEM (ANFIS) :

ANFIS is the fusion of neural network with fuzzy inference system. ANFIS Controller alters PI parameters (K_p,K_i) in accordance with the change in power system operating condition at the time of disturbance. Fuzzy logic is a branch of artificial intelligence, characterized by fuzzification ,defuzzification and rule base . Fuzzy logic deals with linguistic variables and neural network. Requires input and output database for training. Generally, for linear database back propagation network is used and for nonlinear database multilayer feed forward neural network is preferred.

ISSN: 2278-4632
Vol-13, Issue-02, No.01, February 2023

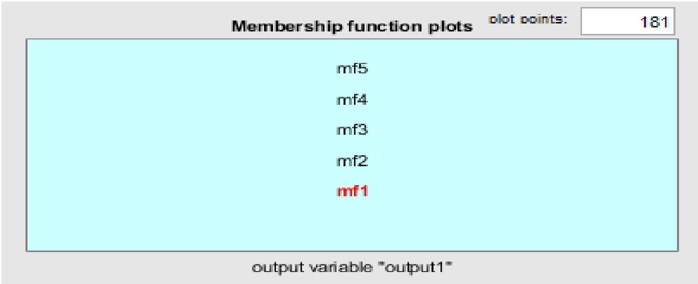

Fig.13: ***Output***

ANFIS Rules:

E/EC	NB	NM	NS	ZE	PS	PM	PB
NB	NB	NB	NB	NB	NM	NS	ZE
NM	NB	NB	NB	NM	NS	ZE	PS
NS	NB	NB	NM	NS	ZE	PS	PM
ZE	NB	NM	NS	ZE	PS	PM	PB
PS	NM	NS	ZE	PS	PM	PB	PB
PM	NS	ZE	PS	PM	PB	PB	PB
PB	ZE	PS	PM	PB	PB	PB	PB

E =Error
EC= Change in Error
NB= Negative Big
NM=Negative Medium
NS= Negative Small
ZE=Zero
PB=Positive Big
PM=Positive Medium
PS=Positive Small

Table.2 ANFIS Rules

The variables for input Membership Function (MF) are Negative Big (NB),Negative Small (NS),Negative Medium (NM),Zero(Z),Positive Small (PS),Positive Medium(PM),Positive Big(PB) as fuzzy subsets. Error (e) / change of error (de) is the input and outputis the desired control signal. Here, three triangular membership functions (MFs) as low, medium and high are considered. After selection of a proper MF for input, the rule base is created and IF…THEN logic is used to create rule base.

Inference is applied to continue with centroid method of defuzzification. After defuzzification, the crisp value is obtained as output. In neural network,weight is updated as per the data rule and training continues till the error becomes zero. Selection of the proper MF will result into the zero error in less number of iterations.

1) STATE 1-SIDO (SINGLE INPUT DUAL OUTPUT) STATE OF THE CONVERTER (POWER TRANSFER FROM PV (VDC) TO LOAD):

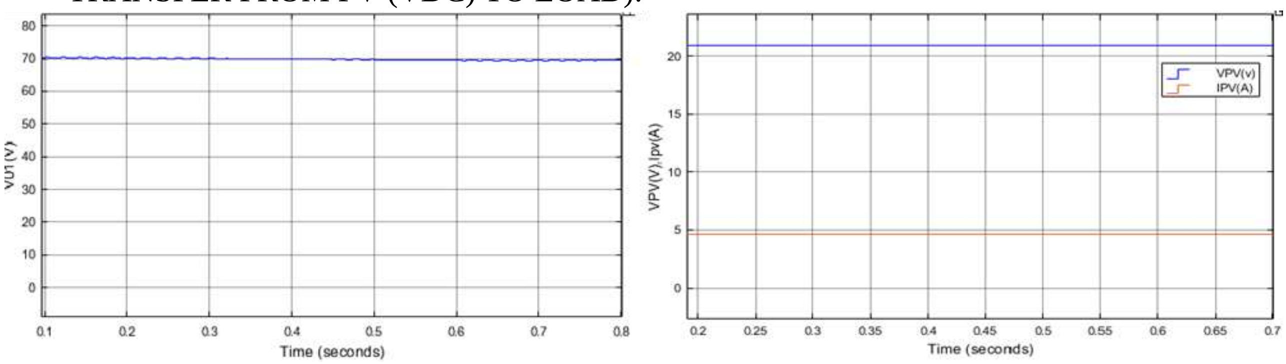

(a) (b)

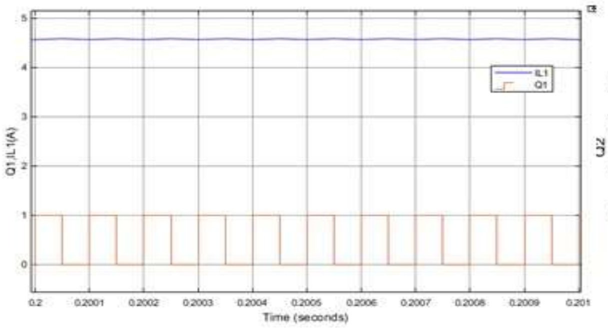

(c)

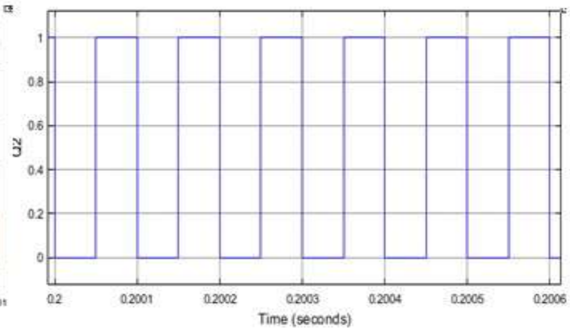

(d)

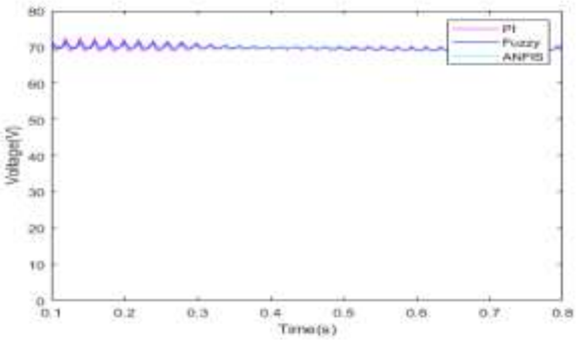

(e)

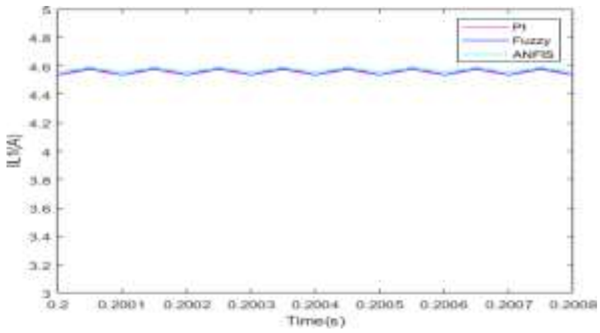

(f)

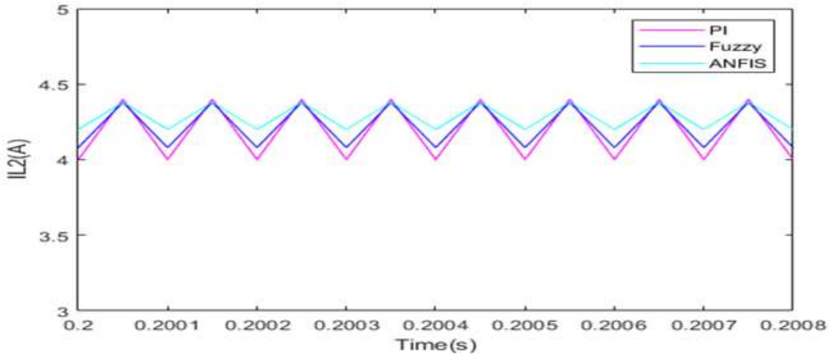

(g)

Fig. 14: (a) $Voltage(V_{01})$; **(b)** $Voltage(V_{pv})$, $Current(I_{pv})$; **(c)** $Inductor\ Current(I_{l1})$; **(d)** $Gate\ Pulse(Q_2)$; **(e)** $Voltage(V_0)$; **(f)** $Inductor\ current(I_{l1})$; **(g)** $Inductor\ Current(I_{l2})$;

2) STATE 2- SITO (SINGLE INPUT THREE OUTPUT) STATE OF THE CONVERTER (POWER TRANSFER FROM PV TO BATTERY AND LOAD):

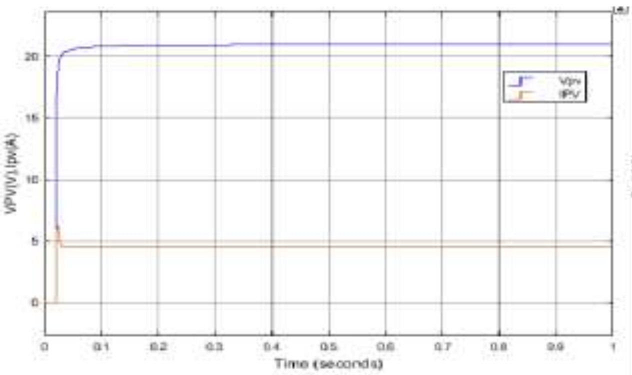

(a)

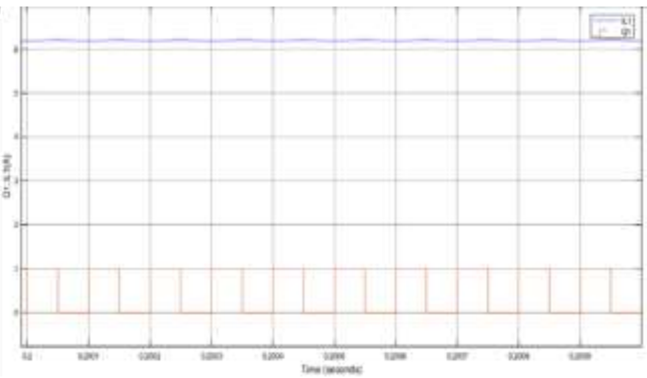

(b)

ISSN: 2278-4632
Vol-13, Issue-02, No.01, February 2023

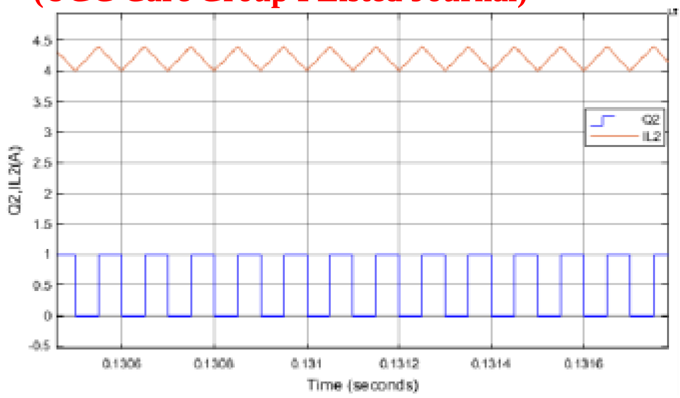

(c)

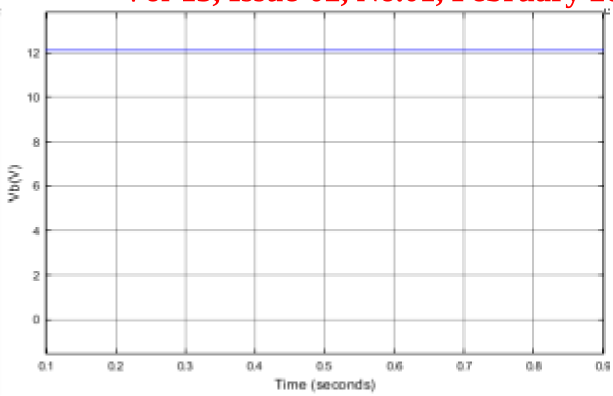

(d)

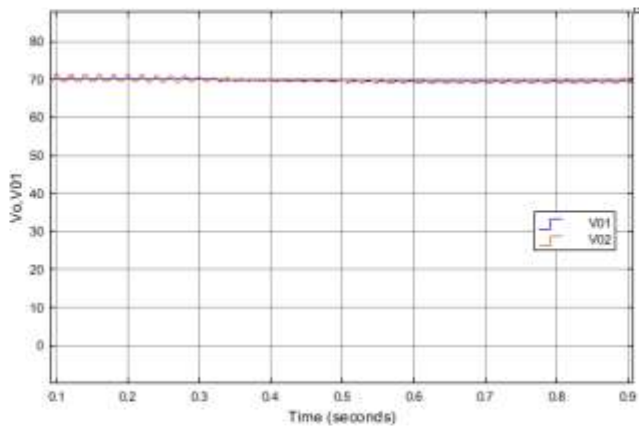

(e)

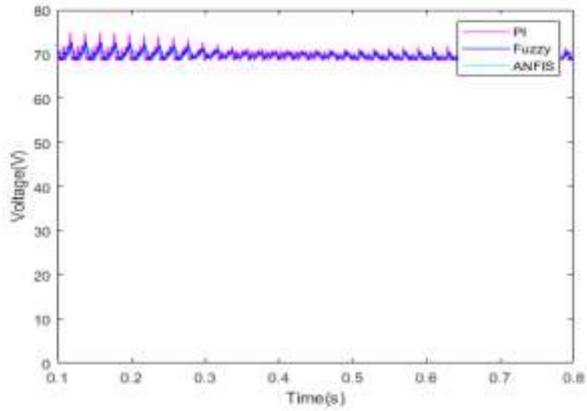

(f)

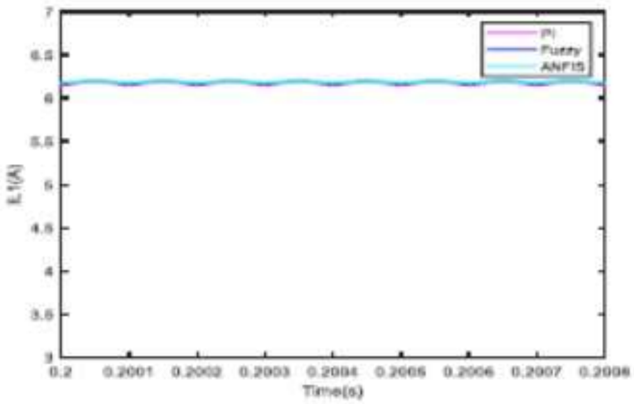

(g)

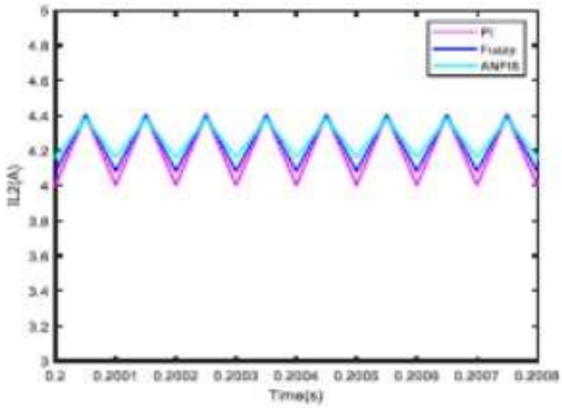

(h)

Fig. 12: (a) $Voltage(V_{pv})$, $Current(I_{pv})$; (b) $Inductor\ Current(I_{l1})$; (c) $Inductor\ current(I_{l2})$; (d) $Battery\ Voltage(V_{bat})$; (e) $Voltages(V_o)$, (V_{01}); (f) $Volatge(V_0)$; (g) $Inductor\ Current(I_{l1})$; (h) $Inductor\ current(I_{l2})$

3) STATE 3 - SIDO STATE OF THE CONVERTER (POWER TRANSFER FROM THE BATTERY)

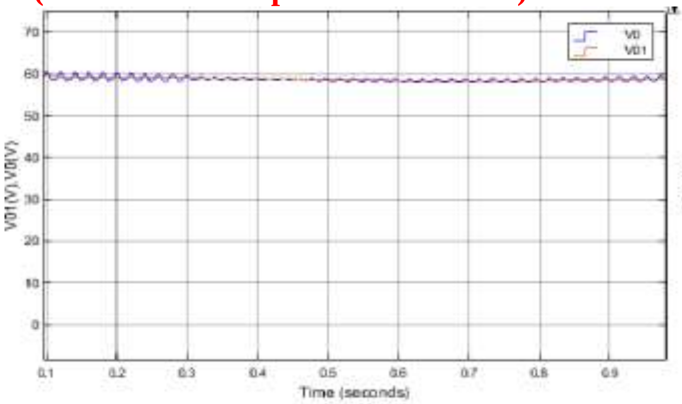

(a)

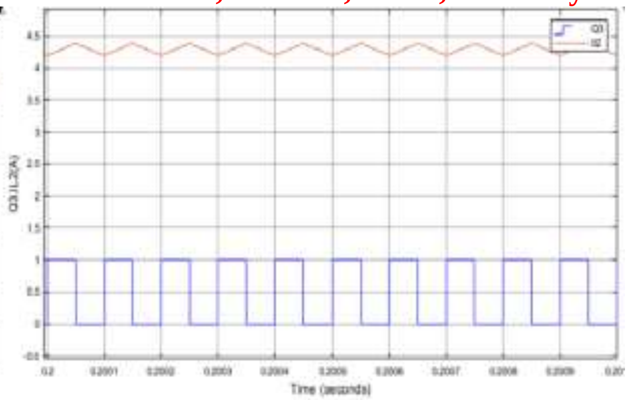

(b)

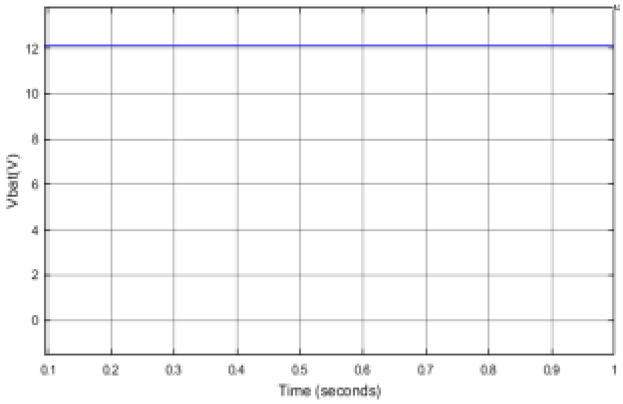

(c)

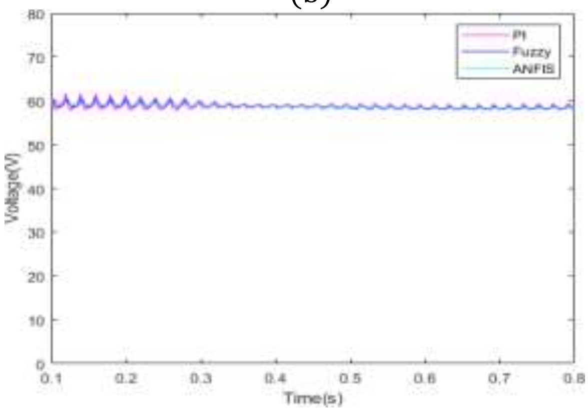

(d)

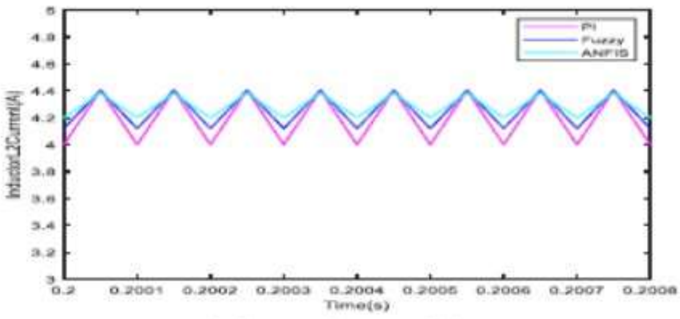

(e)

Fig. 12: (a)$Voltage(V_0)$, (V_{01}); (b) $Inductor\ Current(I_{l2})$; (c) $Battery\ Voltage(V_{bat})$; (d) $Voltage(V_0)$; (e) $Inductor\ Current(I_{l2})$

4) STATE 4 – DIDO (DUAL INPUT DUAL OUTPUT) STATE OF THE CONVERTER (POWER TRANSFER FROM PV AND BATTERY)

ISSN: 2278-4632
Vol-13, Issue-02, No.01, February 2023

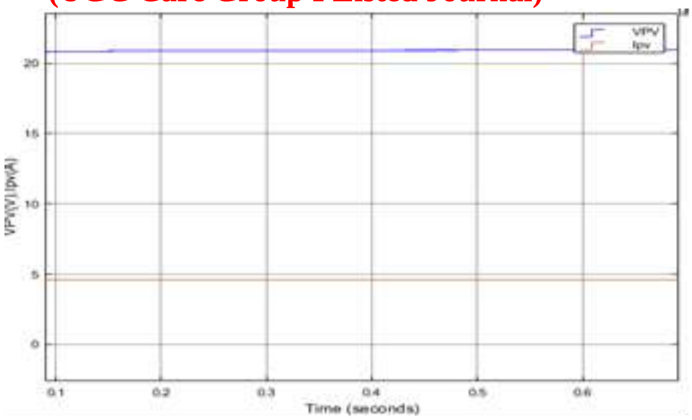

(a)

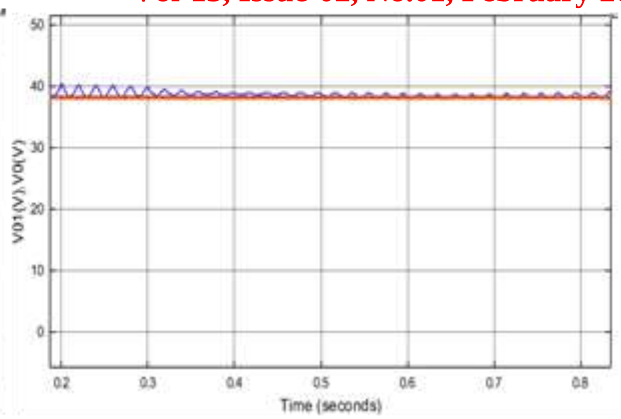

(b)

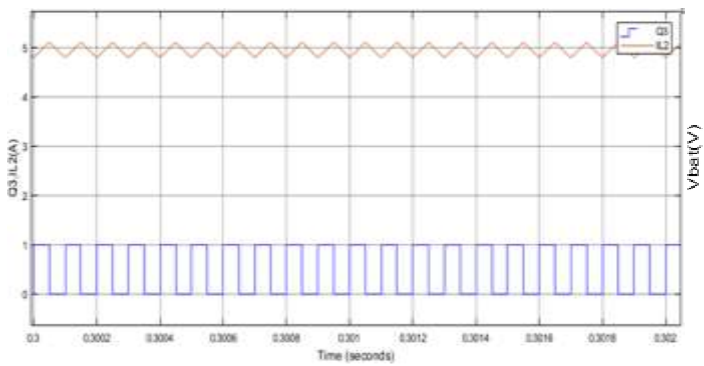

(c)

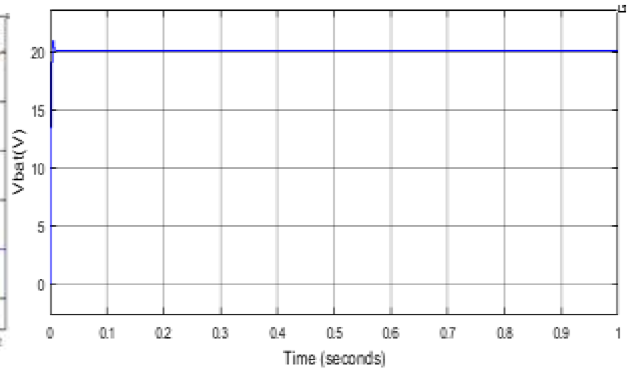

(d)

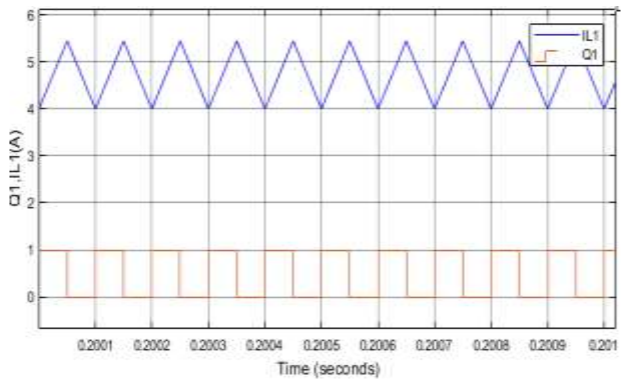

(e)

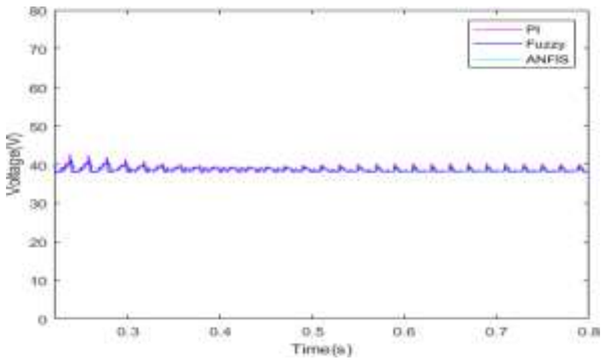

(f)

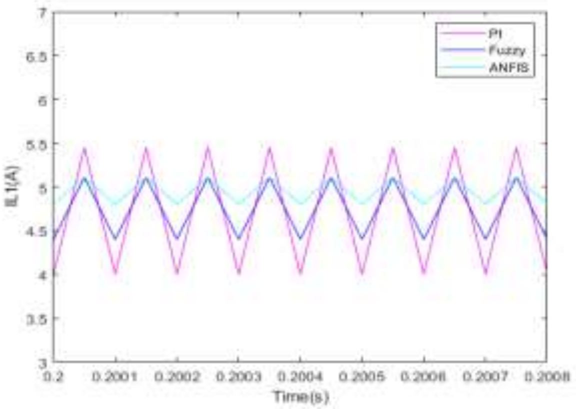

(g)

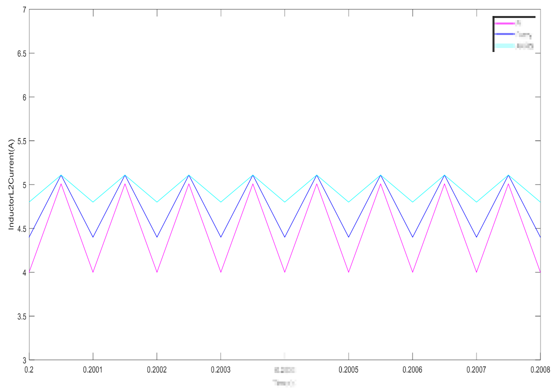

(h)

ISSN: 2278-4632
Vol-13, Issue-02, No.01, February 2023

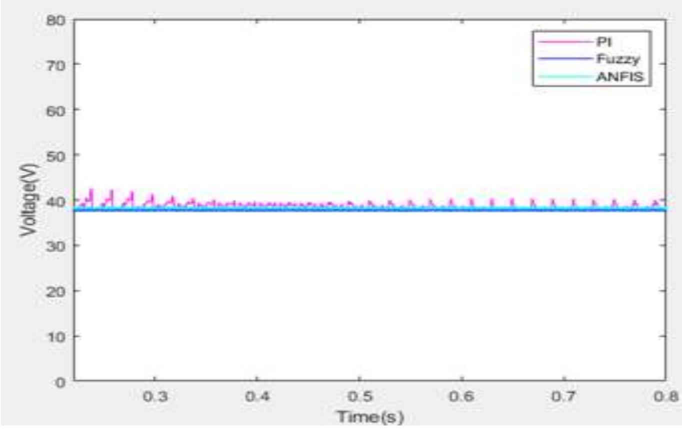

(i)

Fig. 12: (a)$Voltage(V_0)$, (V_{01}); (b) $Inductor\ Current(I_{l2})$; (c) $Battery\ Voltage(V_{bat})$; (d) $Voltage(V_0)$; (e) $Inductor\ Current(I_{l2})$; (f) $Voltage(V_0)$; (g) $Inductor\ Current(I_{l1})$; (h) $Inductor\ Current(I_{l2})$; (i) $Voltage(V_0)$

5) STATE 5 - SIDO STATE OF THE CONVERTER (POWER TRANSFER FROM LOAD TO BATTERY)

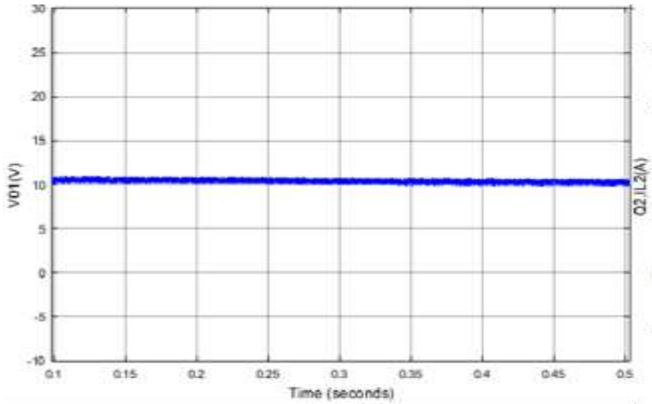

(a)

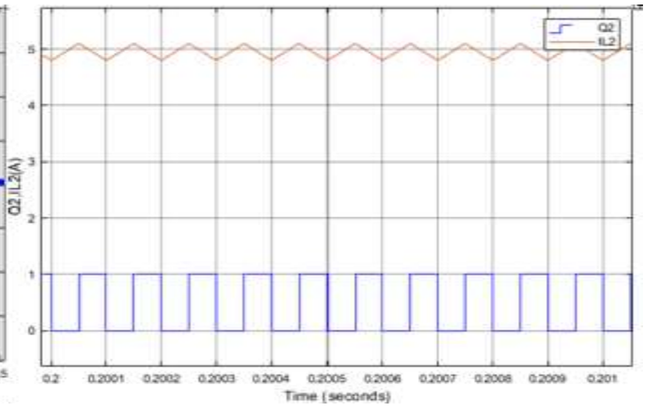

(b)

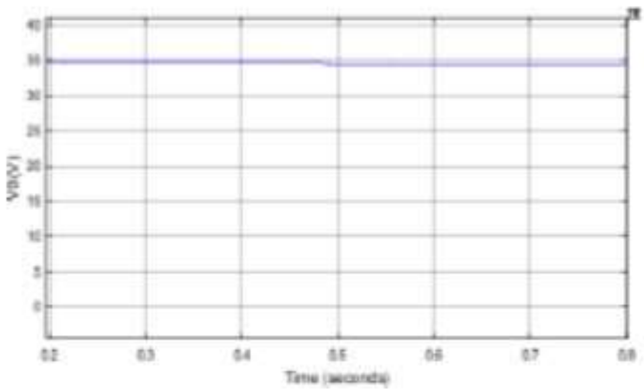

(c)

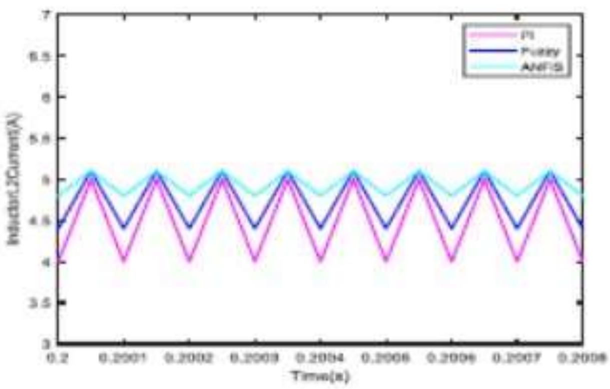

(d)

ISSN: 2278-4632
Vol-13, Issue-02, No.01, February 2023

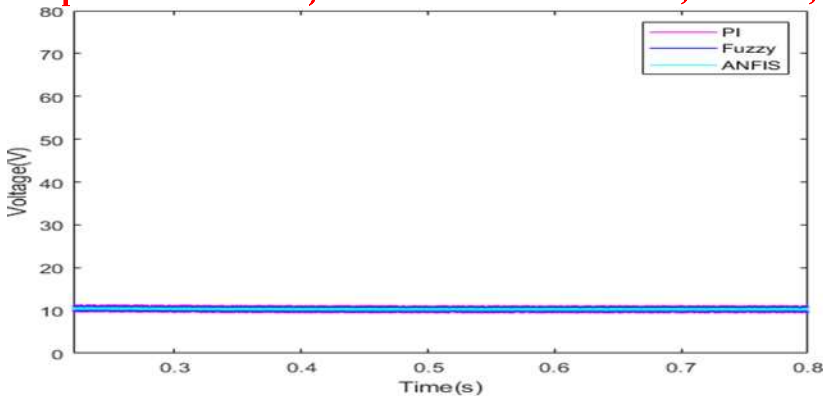

(e)

Fig. 12: (a) $Voltage(V_0)$, (V_{01}); **(b)** $Inductor\ Current(I_{l2})$; **(c)** $Battery\ Voltage(V_{bat})$; **(d)** $Inductor\ Current(I_{l1})$; **(e)** $Voltage(V0)$;

CONCLUSION:

In this project, an ANFIS & Fuzzy Logic Controller is used to implement a modified structure of non isolated, four – port (two input and two output ports) converter, power electronic interfaces for use in electric vehicle (EV) applications. Compared to existing buck boost converter, the Four-port converter (FPC) has the advantages of a)producing buck, boost, buck-boost output even without the use of an additional transformer b)having bidirectional power flow capability with reduced component count c)individual power flow control between the sources d)handling multiple resources of different voltage and current capacity e)easy design, control and implementation process. Compared to PI Controller, the Fuzzy logic controller & ANFIS controller has less oscillations, low steady state error and less harmonic ripples. Compared to PI and Fuzzy controller,ANFIS Controller has good performance ,greater efficiency and it reduces the switching losses.

REFERENCES:

[1] H. Wu, Y. Xing, Y. Xia, and K. Sun, ‘‘A family of non-isolated three-port converters for stand-alone renewable power system,’’ IEEE Trans. Power Electron., vol. 1, no. 11, pp. 1030–1035, 2011.

[2] K. I. Hwu, K. W. Huang, and W. C. Tu, ‘‘Step-up converter combining KY and buck-boost converters,’’ Electron. Lett., vol. 47, no. 12, pp. 722–724, Jun. 2011.

[3] H. Xiao and S. Xie, ‘‘Interleaving double-switch buck–boost converter,’’ IET Power Electron., vol. 5, no. 6, pp. 899–908, Jul. 2012.

[4] H. Kang and H. Cha, ‘‘A new nonisolated High-Voltage-Gain boost converter with inherent output voltage balancing,’’ IEEE Trans. Ind. Electron., vol. 65, no. 3, pp. 2189–2198, Mar. 2018.

[5] T. Bang and J.-W. Park, ‘‘Development of a ZVT-PWM buck cascaded buck–boost PFC converter of 2 kW with the widest range of input voltage,’’ IEEE Trans. Ind. Electron., vol. 65, no. 3, pp. 2090–2099, Mar. 2018.

[6] C.-C. Lin, L.-S. Yang, and G. W. Wu, ‘‘Study of a non-isolated bidirectional DC–DC converter,’’ IET Power Electron., vol. 6, no. 1, pp. 30–37, Jan. 2013.

[7] M. A. Khan, A. Ahmed, I. Husain, Y. Sozer, and M. Badawy, ‘‘Performance analysis of bidirectional DC–DC converters for electric vehicles,’’ IEEE Trans. Ind. Appl., vol. 51, no. 4, pp. 3442–3452, Jul. 2015.

[8] S. Dusmez, A. Khaligh, and A. Hasanzadeh, ‘‘A zero-voltage-transition bidirectional DC/DC converter,’’ IEEE Trans. Ind. Electron., vol. 62, no. 5, pp. 3152–3162, May 2015.

[9] H. Zhu, D. Zhang, B. Zhang, and Z. Zhou, ‘‘A nonisolated three-port DC–DC converter and three-domain control method for PV-battery power systems,’’ IEEE Trans. Ind. Electron., vol. 62, no. 8, pp. 4937–4947, Aug. 2015.

[10] M. B. Camara, H. Gualous, F. Gustin, and A. Berthon, ‘‘Design and new control of DC/DC converters to share energy between supercapacitors and batteries in hybrid vehicles,’’ IEEE Trans. Veh. Technol.,

vol. 57, no. 5, pp. 2721–2735, Sep. 2008.
[11] T. Kim and S. Kwak, ‘‘Single pole switch leg based multi-port converter with an energy storage,’’ IET Power Electron., vol. 9, no. 6, pp. 1322–1330, May 2016.
[12] H. Wu, Y. Lu, L. Chen, P. Xu, X. Xiao, and Y. Xing, ‘‘High step-up/stepdown non-isolated BDC with built-in DC-transformer for energy storage systems,’’ IET Power Electron., vol. 9, no. 13, pp. 2571–2579, Oct. 2016.
[13] A. Ajami, H. Ardi, and A. Farakhor, ‘‘Design, analysis and implementation of a buck-boost DC–DC converter,’’ IET Power Electron., vol. 7, no. 7, pp. 1906–1914, Nov. 2014.